J Mater Sci: Mater Med (2009) 20:387–395
DOI 10.1007/s10856-008-3594-z

Rhodamine-loaded poly(lactic-co-glycolic acid) nanoparticles for investigation of in vitro interactions with breast cancer cells

Tania Betancourt · Kunal Shah · Lisa Brannon-Peppas

Received: 29 May 2008 / Accepted: 10 September 2008 / Published online: 25 September 2008

Abstract Nanoparticle-based drug delivery systems are considered promising for the delivery of imaging agents and drugs for the detection and treatment of illnesses, including cancer. Investigation of nanoparticle interactions with the diseased cells can lead to better designs. In this work, poly(lactic-co-glycolic acid) nanoparticles loaded with rhodamine 6G were prepared by nanoprecipitation with high encapsulation efficiency. In vitro release studies demonstrated that rhodamine escaped from the nanoparticles at a very slow rate at physiological pH, thus making it ideal for imaging studies. At acidic pH this agent was released quickly, suggesting charge interactions between the polymer and rhodamine. Microscopy and flow cytometry studies show higher uptake in MDA-MB-231 breast cancer cells when exposed to rhodamine-loaded nanoparticles than to rhodamine in solution.

1 Introduction

Biodegradable nanoparticles have been recently the focus of research in the delivery of imaging and therapeutic agents as they promise to improve early detection of various diseases, reduce dose-limiting side effects caused by a range of drugs, and improve the efficacy of treatments by controlling the spatial and temporal distribution of the agent or drug in vivo. As drug delivery systems, biodegradable nanoparticles offer benefits including enhanced protection of the active agent from degradation in the physiological environment, maintenance of drug levels within desired therapeutic limits, maximal use of the pharmaceutical, the need for fewer doses, and better patient compliance [1–3]. Because of the great opportunities that nanoparticles offer in diagnostics and treatment, elucidation of the interactions of these systems at the cellular level is of great importance. Better understanding of nanoparticle-cell interface can lead to the design of improved systems.

In this work, the formulation of biodegradable nanoparticles loaded with the fluorescent molecule rhodamine 6G (RHO) was investigated with the purpose creating formulations to be used for study the interactions of the nanoparticles with target cells in vitro through confocal fluorescence microscopy and flow cytometry. The hypothesis here was that these nanoparticles could be used to elucidate the behavior of the formulations containing therapeutic agents in vitro through imaging methods. For this to be true, RHO-loaded nanoparticles must have properties equivalent to the nanoparticles loaded with therapeutic agents, i.e. similar size, morphology, and surface chemistry.

RHO is a fluorescent dye that is commonly used as a label for detection and monitoring of molecules in fluorescence microscopy, flow cytometry, immunohistochemistry and spectroscopy. RHO has a molecular weight of 479 g/mol. RHO is highly soluble in water, ethanol, methanol, acetone and dimethyl sulfoxide, among other agents. It presents absorption and fluorescence peaks at about 530 nm and 550 nm, respectively. RHO has been previously used as a dye for mitochondrial staining and as an inhibitor of mitochondrial function in cells [4, 5], for general cellular staining

T. Betancourt · K. Shah · L. Brannon-Peppas
Department of Biomedical Engineering, The University of Texas at Austin, 1 University Station, Austin, TX 78712, USA

L. Brannon-Peppas (✉)
Appian Labs, LLC, 11412 Bee Caves Road, Suite 300, Austin, TX 78738, USA
e-mail: lpeppas@etibio.com

[6] and also as a dye for imaging of nanoparticles for gene delivery in vivo [7–9].

The biodegradable RHO-loaded nanoparticles were prepared with poly(lactide-co-glycolide) (PLGA), the copolymer of lactide and glycolide. PLGA is a biodegradable polymer that has been clinically used for resorbable sutures as well as in numerous drug delivery systems, including Lupron Depot® formulation of leuprolide acetate for the treatment of prostate cancer and endometriosis (TAP Pharmaceutical Products), Nutropin Depot® formulation of human growth hormone (Genentech), Sandostatin® Depot PLGA microsphere formulation for inhibition of human growth hormone secretion (Novartis), ProLease® (Alkermes) and Trelstar® Depot (Debiopharm) [10, 11]. PLGA is degraded in physiological media by hydrolysis, generating lactic acid and glycolic acid which are further metabolized into carbon dioxide and water in the body [12, 13].

2 Materials and methods

2.1 Materials

Rhodamine-6G (RHO) was obtained from ACROS Organics (Morris Plains, NJ, USA). Bovine serum albumin was obtained from Sigma-Aldrich (Saint Louis, MO, USA). Acetone, methanol and ethyl acetate were obtained from Fisher Scientific (Fairlawn, NJ, USA) and were of HPLC grade. PLGA (formerly PLGA50:50DL2A, now 5050DLGA2A, 50/50 D,L-lactide to glycolide ratio, molecular weight 11,000 g/mol, carboxylic acid and hydroxyl end groups) was obtained from LakeShore Biomaterials (Birmingham, AL, USA).

2.2 Preparation of RHO-loaded nanoparticles

Nanoparticles with RHO were prepared with an oil-in-water nanoprecipitation method [14–16]. RHO was first dissolved in acetone at concentrations ranging from 0.017 to 0.1 mg/ml. A volume of 3–4.35 ml of this solution was then used to dissolve 100 mg of PLGA. This organic solution was then added to 10 ml of an aqueous solution containing 10 mg/ml of bovine serum albumin, vortexed and sonicated for 30 s to form a nanoparticle suspension. Acetone was evaporated by stirring the suspension at 500 rpm under vacuum for 45 min. Nanoparticles were recovered by centrifugation for 10 min at 48,000 × *g* with a refrigerated Beckman J2-21 centrifuge (Beckman Instruments Inc., Palo Alto, CA). The particles were washed three times by resuspending in 10 ml of the surfactant solution through sonication and/or vortexing, followed by centrifugation. Supernatants from each centrifugation were collected for determination of the amount of the imaging agent that had not been encapsulated within nanoparticles. Blank nanoparticles or nanoparticles with no RHO were prepared similarly except that PLGA was directly dissolved in 3 ml of acetone.

Small samples of the nanoparticle suspension were taken throughout the preparation procedure in order to identify and troubleshoot any step at which the particles aggregated. After three washes, the nanoparticle pellet was frozen at −20°C without any cryoprotectant, freeze dried in a Labconco Freeze Dryer 4.5 for 2 days, and stored at −20°C.

2.3 Nanoparticle characterization

The yield of nanoparticle batches was determined by weighing out the mass of dry nanoparticles that was produced after freeze drying and comparing it to the mass of polymer and RHO that was used to prepare the particles. Particle size was determined using a Coulter Nanosizer from suspensions of nanoparticles in water. The Nanosizer uses photon correlation spectroscopy to determine particle size from the temporal variation of light scattering caused by Brownian motion of the suspended particles. Particle sizes were determined during the preparation process by diluting samples of nanoparticle suspensions in deionized (DI) water and after freeze drying by resuspending a small amount of dry nanoparticles in DI water with sonication.

The zeta potential of the nanoparticles was measured with a ZetaPlus® instrument (Brookhaven Instruments Corporation), Holstville, NY, USA). Freeze dried nanoparticles were resuspended by sonication in 1 mM KCl solution at a concentration of 1 mg/ml. Ten zeta potential readings were obtained for each batch.

Nanoparticle morphology was studied through scanning electron microscopy (SEM). A small amount of freeze dried nanoparticles was suspended in DI water with sonication and vortexing and dried at room temperature on top of a carbon conductive tab held on top of a aluminum sample disk holder (Tad Pella Inc., Redding, CA, USA). SEM samples were sputter coated with metal plasma and imaged with a Hitachi 4500 electron microscope.

2.4 Determination of RHO encapsulation efficiency and loading

Encapsulation efficiency (EE), or the percentage of the total amount of imaging agent used in the preparation that was actually encapsulated, was determined by quantifying the amount of agent found in supernatants collected during the cycles of nanoparticle washes ($M_{RHO\text{-}Supernatants}$) and comparing it to the mass of agent used for nanoparticle preparation ($M_{RHO\text{-}Preparation}$), as described in Eq. 1.

$$\mathrm{EE} = \frac{\left(\mathrm{M_{RHO-Preparation}} - \mathrm{M_{RHO-Supernatants}}\right)}{\mathrm{M_{RHO-Preparation}}} \times 100\% \quad (1)$$

The mass of the RHO lost in the supernatants was determined by absorption spectroscopy using standard curves ($r^2 > 0.99$) of known concentrations of the agent in the surfactant solution used for nanoparticle suspension and washing. A Shimadzu UV-1201 UV/Vis spectrophotometer with an optical range from 200 to 1,100 nm was used for this purpose. RHO absorbance was measured at the peak wavelength of 530 nm in bovine serum albumin solution.

Loading, or the weight percent of RHO in the final formulation, was calculated by dissolving a known mass of nanoparticles (M_{NPs}) in dichloromethane, and determining the amount of RHO in solution ($M_{RHO\text{-}IN\text{-}NPs}$) based on a standard curve ($r^2 > 0.99$) of known concentrations of the agent in the same organic solvent. Loading was calculated as described by Eq. 2.

$$\mathrm{Loading} = \frac{\mathrm{M_{RHO-IN-NPs}}}{\mathrm{M_{NPs}}} \times 100\% \quad (2)$$

2.5 In vitro release experiments

The release of RHO under simulated physiological conditions from nanoparticles was studied. A known mass of nanoparticles was suspended in a specific volume of 0.01 M phosphate buffered saline, pH 7.4, and incubated in poly(carbonate) centrifuge tubes in a 37°C water bath. At specific time points, the samples were centrifuged for 15 min at 48,000 × *g* and a portion of the supernatant was removed for analysis and replaced with fresh buffer. Absorption spectroscopy was used to determine the mass RHO released with time. Each set of data was run in independent triplicates. The average and standard deviation between repetitions was determined. At the end of the release study, the nanoparticle suspension was centrifuged and all the supernatant was removed. The nanoparticle pellet was resuspended in water and centrifuged to remove excess buffer salts. The supernatant was again removed and the pellet was freeze dried for determination of remaining dry weight and agent content by spectrophotometry. To investigate the effect of pH on the release profile, identical experiments were carried out in isotonic dimethylglutaric acid buffer pH 4.0.

2.6 Studies of nanoparticle interaction with cancer cells in vitro

In vitro experiments were performed to elucidate the interaction between PLGA nanoparticles and cancer cells. As a model, human mammary gland adenocarcinoma cell line MDA-MB-231 was used. These cells were generously provided by Dr. Dharmawhardane, formerly from the Section of Molecular, Cell and Developmental Biology of The University of Texas at Austin. Cells were incubated at 37°C under a 5% CO_2 atmosphere and maintained with Dulbecco's Modified Eagle Medium (DMEM) supplemented with 10 v/v% fetal bovine serum, 1% HEPES buffer, 1% L-glutamine and 1% sodium pyruvate.

For microscopy studies, cells were seeded in four 6-well plates that contained a pre-sterilized coverslip at a concentration of 300,000 cells per well. A day after seeding, the cell media was replaced with media containing 100 μg/ml of RHO-loaded nanoparticles or the equivalent RHO concentration in solution (0.28 μg/ml) based on actual RHO loading. After a 2 h exposure to the RHO-containing formulations, the media was removed and cells were washed three times with Dulbecco's phosphate buffered saline (DPBS), fixed for 15 min in 3.7% formalin and again washed three times. Coverslips were then mounted onto microscopy slides using Fluoromount-G (Southern Biotech, Birmingham, AL, USA) to protect the samples. Microscopy slides were observed with a Leica SP2 AOBS confocal microscope using laser sources at 476, 488 and 496 nm to excite RHO and detecting the fluorescence signal in the 550–650 nm range. All microscopy gain and offset settings were maintained constant throughout the study.

For flow cytometry studies, cells were seeded at a concentration of 500,000 cells per well in 6-well plates. Growth media was replaced with RHO-containing formulations 24 h after seeding. The tested formulations included RHO-loaded nanoparticles, RHO in solution, blank nanoparticles and DPBS as a control. The concentrations used were 5, 50 and 500 μg/ml in DPBS for nanoparticles. Equivalent RHO solution concentrations of 0.014, 0.14 and 1.4 μg/ml were used based on a nanoparticle loading of 0.28 wt%. After exposure to these formulations for 2, 4 or 8 h, cells were washed three times with DPBS and a cell suspension was created using trypsin/EDTA. Cells suspensions were diluted in growth media to stop the trypsinization process, centrifuged and washed three times with DPBS. Cells were finally resuspended in 1 ml of DPBS without Ca/Mg and immediately analyzed with a FACS Calibur flow cytometer (Beckton & Dickinson, Franklin Lakes, NJ, USA) using a 488 nm laser for excitation of RHO and a band centered at 585 nm for detection of fluorescence. Flow cytometer channel voltage and gain were maintained constant throughout the analysis. Flow cytometry data were processed to remove the events associated to free nanoparticles according to their light scattering properties. From the filtered data, the arithmetic mean of the fluorescence intensity of cells exposed to the various formulations was determined.

2.7 Statistical analysis

Significant difference between the means of sample groups was determined using Student's *t*-test based on a confidence level of 95% ($P < 0.05$). Statistical analysis was performed for sizing, yield, encapsulation efficiency and loading data.

3 Results and discussion

In the present work, PLGA nanoparticles loaded with the fluorescent molecule rhodamine were prepared as tools for the investigation of their interaction with tumor cells in vitro through the use of fluorescence microscopy and flow cytometry. In the past several groups have developed similar model nanoparticles for imaging by fluorescence and electron microscopy, although in most cases the particles used for imaging have not been representative of particles used for drug delivery in terms of their physiochemical properties [17–20]. Such differences can result in different biodistribution and cellular uptake. In addition, few reports have been available on the use of flow cytometry for the study of cell-nanoparticle interaction [21–23].

Because the particles synthesized in the present work are being designed to be ultimately intravenously injected and to circulate in the blood before being deposited into tissue in an in vivo setting, the interaction of the particles with the macrophage phagocytic system is relevant. It is well known that hydrophobic nanoparticles such as those made with PLGA are rapidly opsonized and consequently rapidly removed from the circulation after administration [24–26]. The use of serum proteins such as albumin to mask the surface of particles from recognition by the immune system has been previously suggested as a means to increase their circulation time [27]. However, although the use of surface bound serum proteins can significantly increase residence time in the blood, uptake of the particles by organs with high macrophage density such as the liver, spleen, bone marrow, lymph nodes is still dominant [27]. Nanoparticles can also be modified to include hydrophilic and neutral polymers such as poly(ethylene glycol) (PEG), with or without albumin as a tensioactive agent, in order to delay opsonization and sequestration [28–30]. Our group has reported on the evaluation of a number of strategies for the incorporation of PEG onto PLGA nanoparticles [31]. In the present work and as described below, albumin was included as a beneficial agent for the preparation and stability of the nanoparticles, while also taking into account the fact that its presence on the surface of the particles could delay opsonization in vivo.

One final aspect that must be considered in the development of particles for systemic delivery is the fate of the polymer. The degradation time frame of the PLGA used in the present research is of 2–4 weeks in average, as specified by the manufacturer, although it is known that the rate of degradation is also affected by factors such as the geometry and porosity of the nanoparticles in addition to the molecular weight, monomer ratio or end groups of the polymer. The degradation products of PLGA are lactic and glycolic acid, which are rapidly metabolized by the body through the Krebs cycle [27]. In the case of high localization of the nanoparticles at any specific tissue, an inflammatory response is possible which could result in particle phagocytosis.

3.1 Nanoparticle characterization

RHO nanoparticles were successfully prepared using nanoprecipitation by co-dissolving RHO and PLGA in acetone and precipitating the polymer into nanoparticles in an aqueous phase having bovine serum albumin as a stabilizer. Table 1 summarizes the results of RHO nanoparticle characterization. Batch mass recovery, or yield, ranged in average from 74 to 82% and was not dependent on the loading of RHO. Most of the yield loss can be attributed to difficulties in collecting the dry nanoparticles after freeze drying, although losses could have

Table 1 Properties of rhodamine-loaded poly(lactic-co-glycolic acid) nanoparticles. Values shown are the average ± standard deviation for samples of at least 3 independent batches of a given targeted loading

Targeted rhodamine loading (wt%)	Number of samples	Batch yield (%)	Size before freeze drying (nm)	PI_b	Size after freeze drying (nm)	PI_a	Encapsulation efficiency (%)	Loading (wt%)	Zeta Potential (mV)
0	4	74.1 ± 3.9	293 ± 32	4	332 ± 104	6	–	–	−58.9 ± 0.8
0.08	3	81.5 ± 2.8	376 ± 109	2	300 ± 85	5	89.7 ± 0.4	0.07 ± 0.002	*
0.15	4	82.8 ± 3.6	258 ± 54	3	333 ± 219	4	83.4 ± 7.9	0.15 ± 0.03	*
0.3	4	79.1 ± 7.6	282 ± 63	5	291 ± 51	5	89.9 ± 7.9	0.29 ± 0.01	−54.1 ± 3.2

PI_b—polydispersity index of particle size before freeze drying

PI_b—polydispersity index of particle size after freeze drying

* Not measured

also occurred during nanoparticle preparation and centrifugation steps.

The average nanoparticle size was 300 nm before freeze drying and 314 nm after freeze drying. No statistically significant difference was observed in the average size of the particles loaded with 0.08, 0.15 or 0.30 wt% RHO compared to blank nanoparticles, as expected for particles loaded with relatively small amounts of a small molecular weight drug. No significant differences were observed between the size of samples of a given targeted loading before or after freeze drying ($P >> 0.05$). No aggregation of particles, and consequent increase in the average particle size was observed during the various steps of nanoparticle preparation and washing. The size of the particles after freeze drying indicates that no cryoprotectant is needed for lyophilization of these particles. Our group has published similar results in the preparation of PLGA nanoparticles loaded with the chemotherapeutic agent doxorubicin with BSA as the surface stabilizer [32]. It is possible that excess albumin adsorbed to the surface of the nanoparticles provided cryoprotection during the process of freezing and drying.

The polydispersity index (PI) provides an indication of the variation in the nanoparticle size. This index, as given by the Coulter NanoSizer, ranges from 0 to 9 where a reading of 0 indicates a monodispersed formulation while a polydispersity of 9 represents a distribution in which the ratio of the largest to the smallest particle is of 5 or more. This index, however, cannot be used to quantitatively compare the variability of the particle sizes as a function of loading or other conditions. It is merely gives a qualitative indication of the range in particle sizes. As shown in Table 1, the particle preparation method used in this work resulted in the formation of nanoparticle populations of moderate polydispersity. Also, the polydispersity of the particles ranged from 2 to 5 before freeze drying and between 4 and 6 after freeze drying, suggesting the possibility that some particle aggregation occurred during this process although not statistically significant based on the average particle size.

Figure 1 displays a scanning electron microscopy image of RHO-loaded PLGA nanoparticles. The nanoparticles have a roughly spherical morphology and sizes in the range of 100 and 300 nm, with most particles having a diameter of less than 200 nm. These observations agree with the results described above.

The zeta potential of RHO-loaded nanoparticles with 0.3 wt% loading was of −54 mV. This value was not signicanlty different from that of blank nanoparticles, suggesting that loading of the particles with rhodamine did not notably modify their surface properties. The zeta potential of the batches with intermediate rhodamine loading was not measured. The highly negative nature of the particles is a desired property as it can increase the stability of the nanoparticle suspension through interparticle charge repulsion.

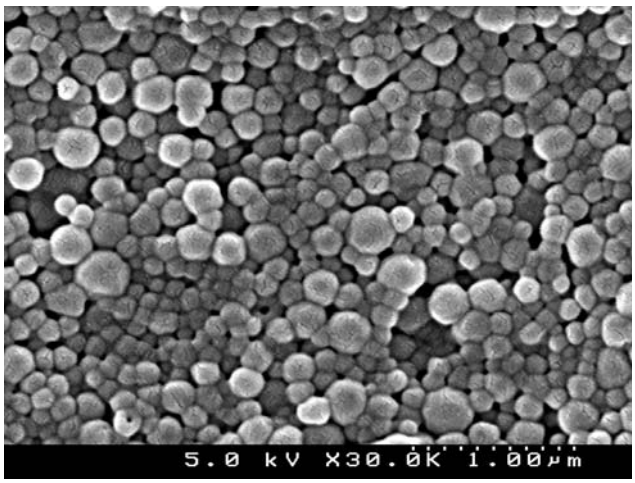

Fig. 1 Scanning electron microscopy image of rhodamine-loaded poly(lactic-co-glycolic acid) nanoparticles. White bar represents a length of 1 µm

The encapsulation efficiency of RHO was in the range of 83–89%. No statistically significant difference was observed between the encapsulation efficiency for the desired loading levels of 0.075, 0.15 or 0.30 wt% RHO. The actual weight percent of RHO that was found to be loaded within dissolved PLGA nanoparticles was within 86% of the targeted loading in all cases. Although higher loading is readily possible since RHO favorably interacts with PLGA, this was not necessary as the particles were already easily detected by fluorescence at the concentration levels tested.

3.2 In vitro release of RHO

In vitro release studies demonstrated that RHO-loaded nanoparticles were an optimal formulation for imaging studies because the hydrophobic RHO was released very slowly, as shown on Fig. 2. Specifically, within 12 h less than 15% of the agent had been released when incubated at 37°C at pH 7.4. On the other hand, at pH 4.0 the nanoparticles rapidly released the agent, with 75% being released within the same 12 h. Acidic pH in the order of 4–5 is typical of lysosomes to which the particles would likely be routed during the process of cellular uptake, while a pH of 7.4 is representative of the extracellular and cytoplasmatic conditions. This pH-dependent release can be associated with charge interactions between the deprotonated PLGA carboxylic acid end groups and the positively-charged RHO at pH 7.4. Such interaction is lost at the acidic pH since then PLGA is in its non-ionic form. In addition, the faster release rate may be associated with

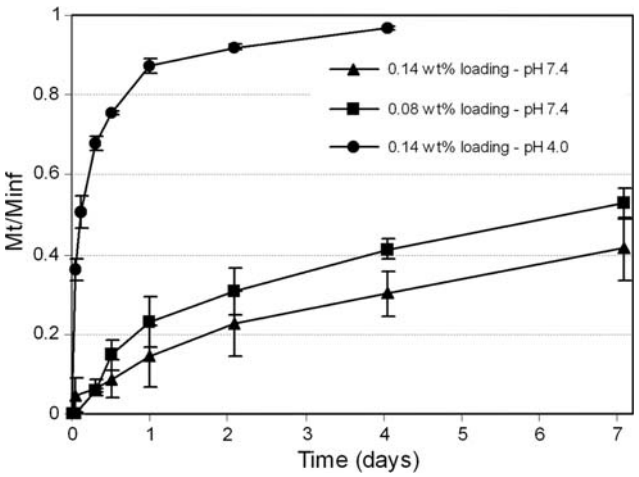

Fig. 2 In vitro release of rhodamine from poly(lactic-co-glycolic acid) nanoparticles as a function of rhodamine loading and pH. The *y*-axis, M_t/M_{inf}, corresponds to the cumulative fraction of rhodamine mass released over time (M_t) compared to the total mass of rhodamine that was released or found in the remaining nanoparticles (M_{inf}). Y bars represent the standard deviation between 3 independent samples for each condition

the faster degradation rate of the polymer at the acidic conditions. Analogous pH-dependent release was observed previously in doxorubicin-loaded PLGA nanoparticles [32], suggesting that this imaging formulation can at least in part simulate the in vitro behavior of therapeutic nanoparticles. Importantly, and as will be described in the next section, controlled release of RHO over a time period of 12 h is more than sufficient for studying the interaction and uptake of nanoparticles by cells in vitro. In addition, and in view of the results, it should be noted that in the event of particle opsonization and sequestration by macrophages, loaded therapeutic or imaging agents would be rapidly released as a result of phagocytosis and consequent enclosure within lysosomes.

3.3 Cellular studies with RHO-loaded nanoparticles

Microscopy and flow cytometry studies of the interaction of RHO-loaded nanoparticles and breast cancer cells were conducted. Microscopy studies, as seen in Fig. 3, show that the cells are able to uptake RHO both when presented in the form of nanoparticles or as a solution. Higher fluorescence intensity, corresponding to higher RHO concentration, was observed in cells exposed to RHO-loaded nanoparticles compared to that in cells exposed to RHO in solution. It is also important to note that RHO fluorescence was distributed throughout the cytoplasm of the cells.

Flow cytometry was used in separate experiments to quantify the level of fluorescence associated with cells treated with the various formulations. For flow cytometry,

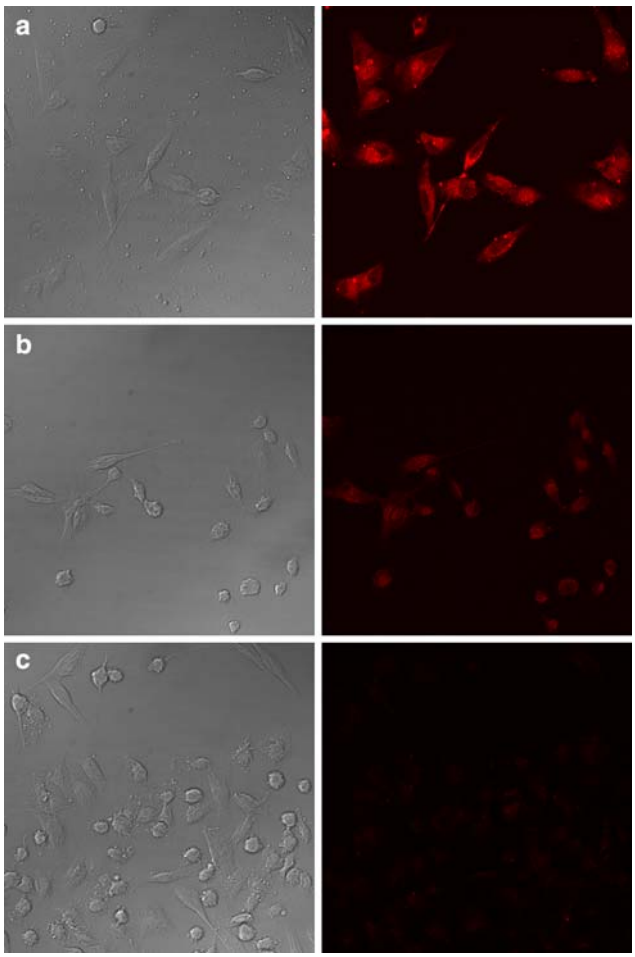

Fig. 3 Confocal microscopy images at the plain of maximum cellular fluorescence of MDA-MB-231 breast cancer cells after exposure to **a** rhodamine-loaded nanoparticles, **b** rhodamine in solution or **c** growth media as a control for 2 h at 37°C. Cells were exposed to 280 ng/ml of rhodamine or to equivalent nanoparticle concentrations based on rhodamine loading

suspensions of blank or RHO-loaded nanoparticles and cells exposed to these formulations were analyzed. In these studies, laser light of a wavelength of 488 nm was focused on a narrow stream of the flowing suspension of nanoparticles, cells or both. Upon interaction of the light with a nanoparticle or cell, the light scattered in line with the laser source (forward scattering) or perpendicular to it (side scattering), and the fluorescence produced by the sample were detected. As expected, nanoparticles resulted in significantly greater side scattering as a result of their high opacity while cells are able to scatter light in the forward direction in a much greater amount as a result of their low index of refractivity. This difference was used to separate the data of independent nanoparticles that had remained in the samples of cells exposed to nanoparticles as the purpose of the experiment was to obtain a quantitative measure of RHO (whether entrapped in nanoparticles, or free) directly

associated with the cells. Figure 4 shows the side and forward scattering of RHO-loaded and blank nanoparticles, and of control and nanoparticle-exposed cells. As shown, clear regions associated with free nanoparticles are visible. Gates were then used to quantify the fluorescence associated with the cells (i.e. for the data points within the high forward scattering and low side scattering region).

After removal of the data of independent nanoparticles, the fluorescence associated which each cell after exposure to RHO in solution or in nanoparticles was determined. Figure 5 shows the arithmetic mean of the fluorescence intensity recorded in the cells exposed to each dosage. As can be seen in both of these figures, the fluorescence associated with cells exposed to RHO-loaded nanoparticles

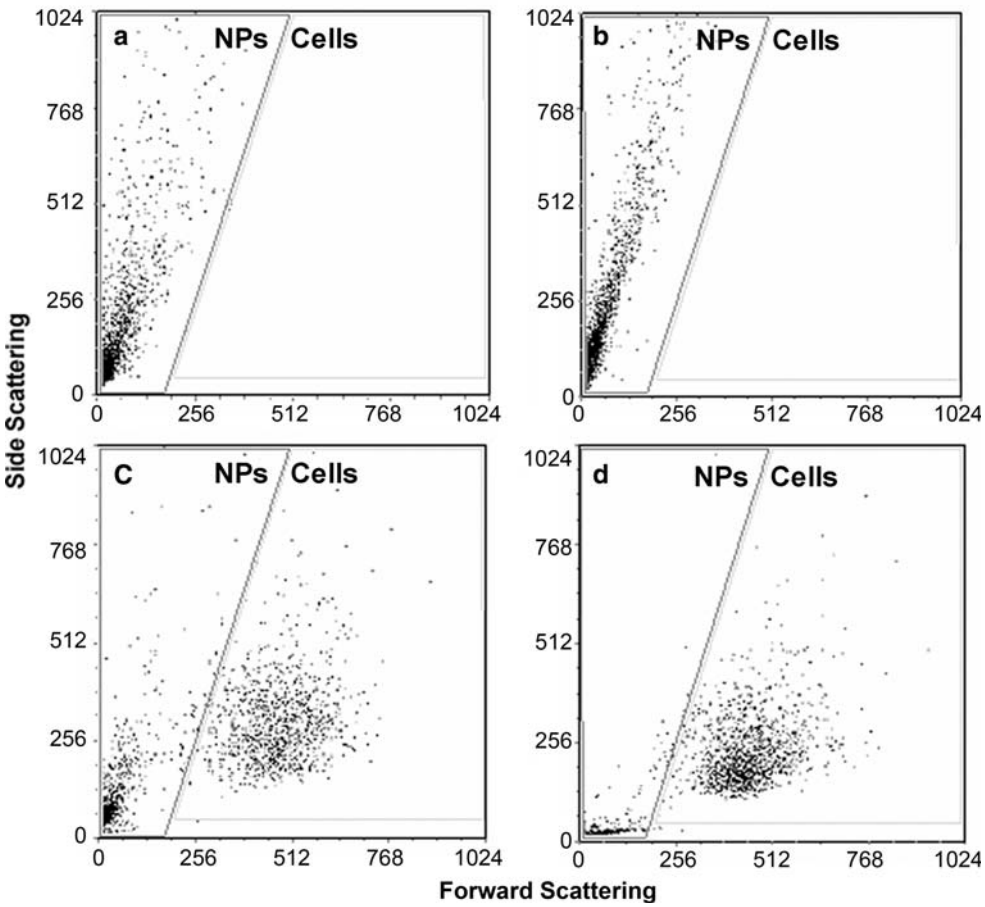

Fig. 4 Plot of forward versus side scattering (*x* and *y*-axis, respectively) of nanoparticle or cell suspensions obtained after flow cytometry analysis. Scattering profile of **a** rhodamine-loaded nanoparticles, **b** blank nanoparticles, **c** MDA-MB-231 breast cancer cells exposed to rhodamine-loaded nanoparticles and **d** control cells. Regions separated by diagonal line on each plot indicate the gates used for separating the data associated with nanoparticles or cells, respectively

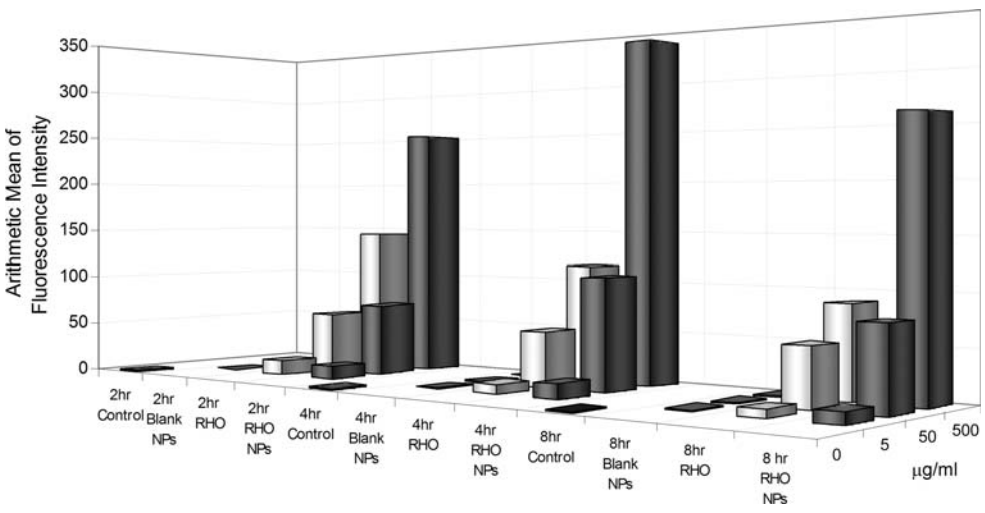

Fig. 5 Arithmetic average of the fluorescence intensity of cells exposed to rhodamine (RHO)-loaded nanoparticles or free RHO in solution for 2, 4 or 8 h obtained by flow cytometry. Fluorescence associated with independent nanoparticles has been removed

was significantly higher than that of cells exposed to RHO in solution for all concentrations and exposure times tested, in accordance to the microscopy results. No fluorescence was detected on cells exposed to blank nanoparticles or to DPBS (control).

Based on the time that RHO-loaded nanoparticles were exposed to the aqueous medium in these in vitro experiments, the fluorescence observed inside of the cells can be attributed to RHO that entered the cells while encapsulated within nanoparticles. From the release profile described in the last section, within the first 8 h only about 10% of the agent would have been released.

The higher RHO cellular uptake by cells in the presence of RHO-loaded nanoparticles compared to RHO in solution, as determined by both microscopy and flow cytometry, may be a result of the high payload of RHO in the nanoparticles. Specifically, based on average particle size, polymer density and RHO loading, each nanoparticle could carry in the range of 59,000 RHO molecules. Consequently, delivery of only a few nanoparticles could lead to high intracellular concentrations. In addition, it is possible that nanoparticle binding and uptake by the cells was mediated by interaction of residual albumin on the surface of the particles and albumin receptors on the cells, thus further increasing the ability of the particles to delivery their payload. These receptors are normally involved in albumin transcytosis across endothelial tissue as have been recently suggested to be participants in the delivery of paclitaxel-albumin bound nanoparticles marketed under the name of Abraxane® [33].

As can be seen in Fig. 5, the fluorescence of cells exposed to RHO in solution appeared to decrease with exposure time. The fluorescence intensity of cells exposed to RHO-loaded nanoparticles increased from 2 to 4 h but appeared to decrease after 8 h of cell exposure. This observation could be a result of cellular efflux mechanisms since RHO molecules have been reported to be substrates for the P-glycoprotein (P-gP) transmembrane receptor associated with multidrug resistance [34, 35]. P-gP is overexpressed in cell lines that are resistant to chemotherapeutic agents, but could be expressed in normal levels by the MDA-MB-231 breast cancer cell line. This cell line is known to be sensitive to chemotherapeutic agents unless specifically adapted to grow under constant chemotherapeutic agent exposure [32, 36, 37].

4 Conclusions

In the present work, a nanoprecipitation technique was utilized for preparation of PLGA nanoparticles loaded with the fluorescent agent RHO. These nanoparticles were designed as models for the study of the interactions of this type of particles with cancer cells by confocal microscopy and flow cytometry. Spherical particles with sizes in the range of 250–350 were prepared with high RHO encapsulation efficiency. Release studies revealed that RHO nanoparticles were optimal for imaging studies because the agent is released at a very slow rate and in a pH-dependent manner as a result of its hydrophobicity and favorable interactions with the polymer. Methods for qualitatively studying the extent of nanoparticle uptake by the cells were described. These methods could be potentially used for the study of the uptake of any type of particle with any time of cell in vitro and even ex vivo. In vitro cellular studies with RHO nanoparticles revealed that MDA-MB-231 breast cancer cells were better able to intake this agent when presented in the form of a nanoparticle suspension rather than as a RHO solution as determined by confocal microscopy and flow cytometry.

Acknowledgements This work was supported in part by the National Science Foundation Integrative Graduate Education and Research Traineeship fellowship to T. Betancourt and The University of Texas at Austin Undergraduate Research Fellowship to K. Shah. We would like to thank the Microscopy and Imaging Facility of the Institute for Cellular and Molecular Biology at The University of Texas at Austin for access to microscopy and flow cytometry equipment.

References

1. L. Brannon-Peppas, Med. Plastics Biomater. Mag. **4**, 34 (1997)
2. J. Panyam, V. Labhasetwar, Adv. Drug Deliv. Rev. **55**(3), 329 (2003). doi:10.1016/S0169-409X(02)00228-4
3. M.D. Wang, D.M. Shin, J.W. Simons, S. Nie, Expert. Rev. Anticancer Ther. **7**(6), 833 (2007). doi:10.1586/14737140.7.6.833
4. A.R. Gear, J. Biol. Chem. **249**(11), 3628 (1974)
5. S. Hu, H. Zhao, X. Yin, J. Ma, J. Toxicol. Environ. Health A **70**(17), 1403 (2007). doi:10.1080/15287390701251990
6. H.W. Tang, X.B. Yang, J. Kirkham, D.A. Smith, Anal. Chem. **79**(10), 3646 (2007). doi:10.1021/ac062362g
7. R.A. Bejiani, D. BenEzra, H. Cohen, J. Rieger, C. Andrieu, J.C. Jeanny et al., Mol. Vis. **11**, 124 (2005)
8. A. Vila, A. Sanchez, C. Evora, I. Soriano, J.L. Vila Jato, M.J. Alonso, J. Aerosol. Med. **17**(2), 174 (2004). doi:10.1089/089426804145718 3
9. A. Vila, H. Gill, O. McCallion, M.J. Alonso, J. Control. Release **98**(2), 231 (2004). doi:10.1016/j.jconrel.2004.04.026
10. M.S. Shive, J.M. Anderson, Adv. Drug Deliv. Rev. **28**(1), 5 (1997). doi:10.1016/S0169-409X(97)00048-3
11. O. Dechy-Cabaret, B. Martin-Vaca, D. Bourissou, Chem. Rev. **104**(12), 6147 (2004). doi:10.1021/cr040002s
12. L. Brannon-Peppas, Int. J. Pharm. **116**(1), 1 (1995). doi:10.1016/0378-5173(94)00324-X
13. D.H. Lewis, Controlled Release of Bioactive Agents from Lactide/Glycolide Polymers, in *Biodegradable Polymers as Drug Delivery Systems*, ed. by M. Chasin, R. Langer (Marcerl Dekker, New York, 1990), p. 1
14. L. Peltonen, P. Koistinen, J. Hirvonen, S.T.P. Pharma. Sci. **13**(5), 299 (2003)
15. H. Fessi, J.P. Devissaguet, F. Puisieux, Thies C. *Procédé de préparation des systèmes colloïdaux dispersibles dune substance*

sous forme de nanoparticules, F·P. Application, Editor (1986) French
16. J.M. Barichello, M. Morishita, K. Takayama, T. Nagai, Drug Dev. Ind. Pharm. **25**(4), 471 (1999). doi:10.1081/DDC-100102197
17. W. Zauner, N.A. Farrow, A.M. Haines, J. Control. Release **71**(1), 39 (2001). doi:10.1016/S0168-3659(00)00358-8
18. D.P. McIntosh, X.Y. Tan, P. Oh, J.E. Schnitzer, Proc. Natl. Acad. Sci. USA **99**(4), 1996 (2002). doi:10.1073/pnas.251662398
19. J. Panyam, S.K. Sahoo, S. Prabha, T. Bargar, V. Labhasetwar, Int. J. Pharm. **262**(1–2), 1 (2003). doi:10.1016/S0378-5173(03)00295-3
20. Y. Zhang, M.K. So, J. Rao, Nano Lett. **6**(9), 1988 (2006). doi:10.1021/nl0611586
21. W. Meng, T.L. Parker, P. Kallinteri, D.A. Walker, S. Higgins, G.A. Hutcheon et al., J. Control. Release **116**(3), 314 (2006). doi:10.1016/j.jconrel.2006.09.014
22. A. Yang, L. Yang, W. Liu, Z. Li, H. Xu, X. Yang, Int. J. Pharm. **331**(1), 123 (2007). doi:10.1016/j.ijpharm.2006.09.015
23. D.W. Bartlett, M.E. Davis, Bioconjug. Chem. **18**(2), 456 (2007). doi:10.1021/bc0603539
24. L. Brannon-Peppas, J.O. Blanchette, Adv. Drug Deliv. Rev. **56**(11), 1649 (2004). doi:10.1016/j.addr.2004.02.014
25. F. Fawaz, F. Bonini, M. Guyot, A.M. Lagueny, H. Fessi, J.P. Devissaguet, Pharm. Res. **10**(5), 750 (1993). doi:10.1023/A:1018924219540
26. K. Avgoustakis, Curr. Drug Deliv. **1**(4), 321 (2004). doi:10.2174/1567201043334605
27. D.V. Bazile, C. Ropert, P. Huve, T. Verrecchia, M. Marlard, A. Frydman et al., Biomaterials **13**(15), 1093 (1992). doi:10.1016/0142-9612(92)90142-B
28. K. Avgoustakis, Curr. Drug Deliv. **1**(4), 321 (2004). doi:10.2174/1567201043334605
29. H. Otsuka, Y. Nagasaki, K. Kataoka, Adv. Drug Deliv. Rev. **55**(3), 403 (2003). doi:10.1016/S0169-409X(02)00226-0
30. S. Stolnik, S.E. Dunn, M.C. Garnett, M.C. Davies, A.G.A. Coombes, D.C. Taylor et al., Pharm. Res. **11**(12), 1800 (1994). doi:10.1023/A:1018931820564
31. T. Betancourt, J.D. Byrne, N. Sunaryo, S.W. Crowder, M. Kadapakkam, S. Patel, et al. J. Biomed. Mater. Res. (in press)
32. T. Betancourt, B. Brown, L. Brannon-Peppas, Nanomedicine **2**(2), 219 (2007). doi:10.2217/17435889.2.2.219
33. M.R. Green, G.M. Manikhas, S. Orlov, B. Afanasyev, A.M. Makhson, P. Bhar et al., Ann. Oncol. **17**(8), 1263 (2006). doi:10.1093/annonc/mdl104
34. J.G. Sarver, W.A. Klis, J.P. Byers, P.W. Erhardt, J. Biomol. Screen. **7**(1), 29 (2002)
35. A. Yoshimura, N. Shudo, S.I. Ikeda, M. Ichikawa, T. Sumizawa, S.I. Akiyama, Cancer Lett. **50**(1), 45 (1990). doi:10.1016/0304-3835(90)90177-Y
36. S.L. Schneider, S.A. Fuqua, K.V. Speeg, A.K. Tandon, W.L. McGuire, In vitro Cell Dev. Biol. **26**(6), 621 (1990). doi:10.1007/BF02624212
37. M. de la Torre, X.Y. Hao, R. Larsson, P. Nygren, T. Tsuruo, B. Mannervik et al., Anticancer Res. **13**(5A), 1425 (1993)